

Enhancing Depth Completion with Multi-View Monitored Distillation

Jia-Wei Guo¹, Cong Li¹, Sen-Hua Zhu², Chang-Zheng Zhang², Ming Ouyang², Ning Ding³, Hung-Chyun Chou¹

Abstract—This paper presents a novel method for depth completion, which leverages multi-view improved monitored distillation to generate more precise depth maps. Our approach builds upon the state-of-the-art ensemble distillation method, in which we introduce a stereo-based model as a teacher model to improve the accuracy of the student model for depth completion. By minimizing the reconstruction error for a given image during ensemble distillation, we can avoid learning inherent error modes of completion-based teachers. To provide self-supervised information, we also employ multi-view depth consistency and multi-scale minimum reprojection. These techniques utilize existing structural constraints to yield supervised signals for student model training, without requiring costly ground truth depth information. Our extensive experimental evaluation demonstrates that our proposed method significantly improves the accuracy of the baseline monitored distillation method.

I. INTRODUCTION

Scene depth perception has found numerous applications in fields such as automatic driving, robotics, and augmented reality [1, 2, 3]. Various sensors, such as LiDAR, RGB-D and stereo cameras, can provide scene depth information [1, 4, 5]. However, these sensors have several limitations, including high costs, limited measurement distance, and high power consumption. In recent years, there has been an increasing focus on learning-based depth estimation, which has led to the development of many efficient and accurate technologies [4, 6, 7]. One of the most popular research directions in deep learning is depth completion, which aims to estimate dense pixel-wise depth from an extremely sparse map obtained by a depth sensor [8, 9].

Deep learning-based methods for depth completion have shown remarkable performance and led to a development trend in recent years. Prior works have used convolutional networks [10] or simple auto-encoders [11] trained on a dataset of images and corresponding sparse depths to complete missing depth information. A traditional method in this category is to use dual encoders to extract detailed features

from an RGB image and its corresponding sparse depth map and then fuse them using a decoder [12, 13]. Recent research on depth completion tends to use more complex network architectures and learning strategies. In addition to feature fusion from images and sparse depth, researchers have begun to introduce surface normal [14], affinity matrix [15], residual depth maps [16], and other techniques into their methodologies. To deal with the lack of supervised pixels, some researchers have focused on knowledge distillation [17], multi-view geometric constraints [18, 19], and adversarial regularization [20]. For example, in [21], a blind ensemble distillation of teacher models was used to generate a distilled depth map with minimum reconstruction error and a confidence map, which can be used to train more accurate student models by selectively learning the best pixel-wise depth estimation from the ensemble and avoiding learning the teachers' error modes.

When the procedure of assembling teachers' results yields high photometric reprojection errors, the student can only rely on unsupervised losses to obtain the correct model parameters. To resolve this, a novel stereo-based teacher is introduced to provide supervised signals for the student's training. Additionally, the method leverages multi-view depth consistency between time-sequential frames to further enhance the student's model convergence. The training process is improved by incorporating multi-scale minimum reprojection among decoder layers. Experimental evaluations on the KITTI benchmark dataset demonstrate the effectiveness of the proposed method, which outperforms state-of-the-art depth completion methods across four metrics.

II. RELATED WORKS

A. Learning-Based Stereo Estimation

Stereo estimation algorithms commonly rely on computing the similarity between corresponding pixels in a calibrated stereo image pair to infer depth information. This process allows for a 1-D search to estimate the disparity, or scaled inverse depth, between the two images. In recent years, learning-based approaches have become popular for stereo estimation, which typically involves four key steps: matching cost computation, cost aggregation, optimization, and disparity refinement.

Traditionally, stereo estimation studies have focused on computing the matching cost using convolution layers and then refining the disparity result using semi-global matching (SGM) [22]. However, more recently, end-to-end networks have been developed that can predict whole disparity results without the need for an explicit feature-matching module or post-processing [23, 24]. For example, PSM-Net [25] proposed an end-to-end deep learning framework for its stereo

*This work was supported by National Key R&D Program of China No. U2013202 and the Guangdong Basic and Applied Basic Research Foundation under Grant No. 2022A1515011139. Corresponding author: Hung-Chyun Chou, Email: zhouhongjun@cuhk.edu.cn

Authors 1 are with Special Robot Center, Shenzhen Institute of Artificial Intelligence and Robotics for Society, 14-15F, Tower G2, Xinghe World, Rd Yabao, Longgang District, Shenzhen, Guangdong, 518129, China.

Authors 2 are with Huawei Cloud Computing Technology Co., Ltd.

Author 3 is with Shenzhen Institute of Artificial Intelligence and Robotics for Society, and Institute of Robotics and Intelligent Manufacturing, The Chinese University of Hong Kong, Shenzhen, Shenzhen, Guangdong, 518172, China.

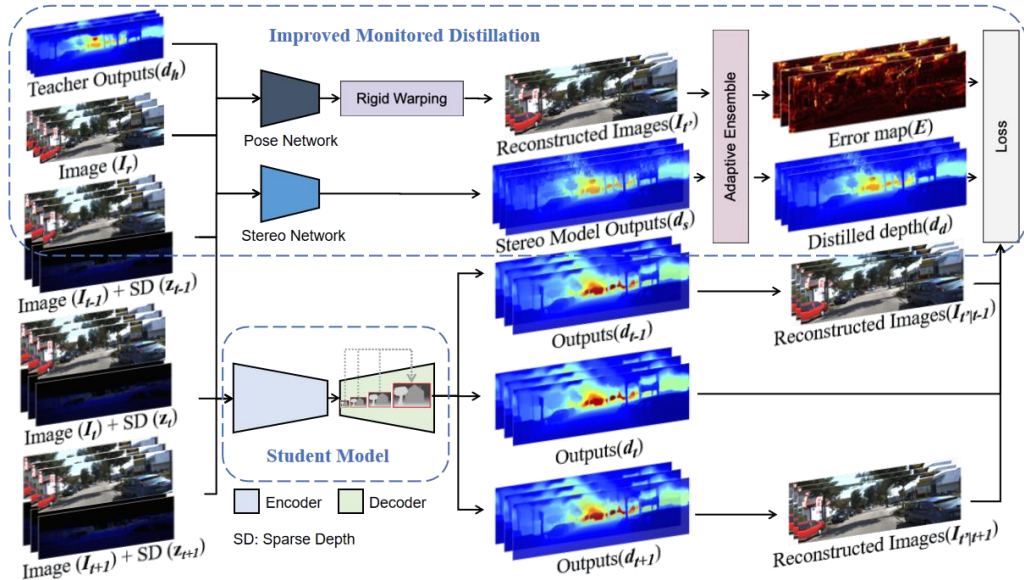


Figure 1. The framework of improved monitored distillation.

matching that does not require post-processing. It introduced a pyramid pooling module into the image features, which further incorporates global context information to improve feature extraction accuracy. In our work, we utilize a stereo-based learning model to enhance the accuracy of supervised information during monitored knowledge distillation.

B. Unsupervised Depth Completion

Typical supervised depth completion methods require ground truth information as supervised signals for model training, which can be difficult to obtain. On the other hand, unsupervised depth completion methods use inherent structure cues related to the pose between adjacent images to improve model accuracy during training. Most of these methods focus on minimizing photometric errors between input images and their corresponding synthetic images reconstructed from different views, or the difference between the estimation and sparse depth, by designing suitable losses [12, 18, 19]. Other researchers have used synthetic data to learn priors on the shapes populating a scene [26, 27].

However, the accuracy of structure information is crucial for achieving better depth completion accuracy during training. To address this, we propose using multi-view depth consistency to supervise the model training, which not only enhances the depth completion accuracy but also improves the accuracy of structure information during training.

C. Knowledge Distillation

Knowledge distillation is a method that utilizes a simpler student model to learn from a larger, more complex teacher model under teacher's supervision. This method has been applied to depth estimation with effective results in recent research [28, 29]. For example, [1] used cycle inconsistency and knowledge distillation for unsupervised monocular depth estimation, where the student network is a part of the teacher network. Additionally, [21] leveraged ensemble learning to adaptively select the best pixel-wise depth result from each

teacher model and avoid learning error modes from these models.

In this paper, we draw inspiration from [18, 21] and propose the use of multi-scale minimum reprojection to further enhance the accuracy of monitored distillation for depth completion without requiring additional inputs.

III. PROPOSED METHOD

A. Overview

This work focuses on the problem of obtaining a dense depth map of a scene from a single image and its corresponding sparse depth map. To address this problem, we propose a depth completion function that takes as input an RGB image I_t , its sparse depth map z_t , and the corresponding camera intrinsics K_t , and outputs a dense depth map d_t . The function aims to learn the underlying mapping between the input and output data by leveraging the inherent structure cues present in the scene.

$$d_t := f_{\theta}(I_t, z_t, K_t) \in \mathcal{R}^{H \times W} \quad (1)$$

During the training phase, we assume access to a set of synchronized image-depth pairs $\{I_i, z_i\}$, where I_i corresponds to a set of temporally adjacent images $[I_{t-1}, I_t, I_{t+1}]$, and z_i denotes the corresponding sparse depth map for each image. In addition, we have access to the corresponding image I_r that is registered with image I_t , which enables us to use stereo-based depth estimation techniques. Furthermore, we assume that a set of N teacher depth outputs $\{d_h^i\}$, $i \in N$ related to image I_t is available from publicly pre-trained models. During training, we input synchronized pairs of images and sparse depth maps into the student model, which outputs a set of dense depth maps $\{d_i\}$, where i corresponds to the temporal index of the input image, i.e., $i \in [t-1, t, t+1]$. The student model employs the depth completion function described in equation (1) to generate the dense depth maps. Meanwhile, we generate reconstructed images I_r^i corresponding to I_t by applying an image warping function.

$$I_t^j = f_\omega(I_t, d_h^i) \quad (2)$$

The photometric reprojection error between I_t and I_t^j is utilized to generate a set of error maps E^i . Then, these error maps can be used to validate the correctness of teacher outputs $\{d_h^i\}$. By selecting the best pixel-wise values with the highest confidence from $\{d_h^i\}$ adaptively, we can construct the distilled depth d_d from these error maps. After that, we update the distilled depth by comparing the confidence of depth values with stereo outputs d_s from stereo-based depth model estimation.

During the training phase, we incorporate multi-view depth consistency by utilizing the depths from adjacent frames (d_{t-1} , d_t , d_{t+1}) to supervise the student model. This approach helps to improve both the accuracy of depth completion and structure information simultaneously. Furthermore, we introduce the multi-scale minimum reprojection to enhance the monitored distillation for depth completion accuracy without requiring any additional inputs.

B. Stereo Constraint Supervision

In the monitored distillation module, we leverage depth completion models as teachers for depth distillation, as proposed in [21]. To further enhance the accuracy of distilled depth in knowledge distillation, we incorporate a stereo-based end-to-end depth estimation model [25]. This model takes in a pair of left-right RGB images and outputs a dense depth map d_s by minimizing an energy function in equation (3) to obtain a disparity map D .

$$E(D) = \sum C(x, d_x) \quad (3)$$

Here, $C(x, d_x)$ represents the matching cost of pixel $x = (i, j)$ in the left image with its corresponding pixel $y = (i, j - d_x)$ in the right image, where $d_x = D(x)$ is the disparity at pixel x . As stereo-based methods use unique feature extraction and fusion using rich texture information from both left and right images, they can often produce more accurate depth values than depth completion methods, especially for scene details. Figure 2 shows that the depth output from the stereo-based method is smoother than that from the depth completion method. Therefore, we leverage the stereo outputs d_s to update the distilled depth d_d through comparing the confidence of depth values.

$$d_d^j = d_s^i \text{ if } E_d^j < E_s^i \quad (4)$$

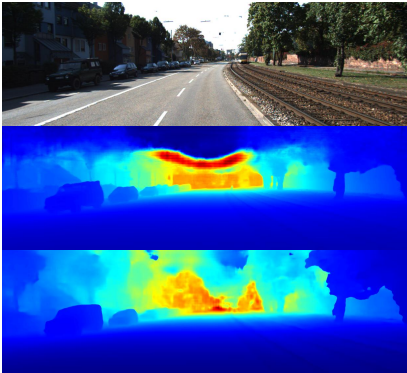


Figure 2. Depth outputs from depth completion method (middle) and stereo-based method (bottom).

C. Multi-view Depth Consistency

Many existing depth estimation methods do not take into account the depth consistency between all adjacent views. In our proposed approach, we aim to incorporate this information by inputting both the current image and its all adjacent images into the student model during training. This results in the generation of the corresponding depth outputs $\{d_i\}$, $i \in [t-1, t, t+1]$. These depth outputs are then used to reconstruct their corresponding adjacent views through the warping function. To further improve the accuracy of our approach, we construct photometric and structure loss functions that calculate the errors between all reconstructed adjacent images.

$$L_{photometric} = \sum (|I_x - I_{x|y}|) \quad (5)$$

$$L_{structure} = \sum (1 - \psi(I_x, I_{x|y})) \quad (6)$$

Here, $x, y \in [t-1, t, t+1]$, $x \neq y$ and ψ represents structural similarity index distance, SSIM. Due to the fact that student network and pose network are responsible for the errors, the errors can be supervision information to supervise model training for better accuracy of depth completion. This is particularly useful when the monitored teacher distillation results in undesirable depth output with low confidence values [21]. Furthermore, the photometric and structure loss functions used for calculating these errors can also improve the accuracy of structure information during training.

D. Multi-scale Minimum Reprojection

Inspired by techniques for improving depth quality [18], we incorporate multi-scale reprojection supervision into the loss function during depth model training. The approach involves upsampling the lower resolution depth outputs, which are the intermediate outputs, to match the input image resolution. Based on equations (2), (5) and (6), we then calculate the photometric and structure error between the upsampled depth outputs and the highest resolution views. This process is depicted in Figure 3. This method is similar to matching patches, meaning low-resolution disparity values are responsible for reconstructing certain blocks of pixels in the highest resolution image directly. This approach helps each scale resolution layer converge towards accurately reconstructing the highest resolution target image, improving the overall quality of the depth output.

In order to reduce the influence of occluded pixels, which may cause high photometric error in multi-view feature matching, we introduce the minimum operation into the photometric and structure loss over all adjacent images. This operation is applied to the per-pixel photometric and structure loss, as defined in equations (5) and (6), to obtain the final loss functions given by equations (7) and (8), respectively. The minimum operation selects the smallest loss value among the adjacent views for each pixel, which helps to avoid the negative influence of occlusion on the loss calculation and thus improves the accuracy of the depth estimation.

$$L_{photometric} = \sum (\min_{\text{per-pixel}} |I_x - I_{x|y}|). \quad (7)$$

$$L_{structure} = \sum (1 - \min_{\text{per-pixel}} (\psi(I_x, I_{x|y}))). \quad (8)$$

IV. EXPERIMENTS

We evaluate the performance of our proposed method using publicly available benchmarks and compare it with previously published methods. Our experiments are conducted without access to ground truth during the training phase.

A. Experimental Setup and Benchmark

We conduct experiments on the large-outdoor KITTI driving datasets, which comprise approximately 86,000 raw 1242x375 image frames and their corresponding synchronized sparse depth maps. These images were captured using two video cameras and a LiDAR sensor, with the valid area of sparse depth covering only about 5% of the image space. To validate our approach, we use 1,000 designated samples and their corresponding ground truth depths, along with semi-dense data.

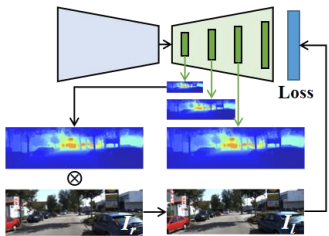


Figure 3. Multi-scale photometric reprojection.

For our distillation models, we adopt the approach of [21] and use PENet [30], MSG_CHN [31], ENet [30], and NLSPN [32] as depth completion teacher ensembles. Additionally, we introduce PSMNet [25] as a stereo-based depth estimation teacher to further improve our distillation method. We evaluate the performance of our proposed method quantitatively using several metrics commonly used in previous works [21], as presented in Table 1. Here, we define P as the total number of pixels in the test maps and d_e and d_{gr} as the estimated depth and ground truth depth, respectively.

Table 1. Evaluation metrics.

Metric	Definition
MAE	$(\sum d_e - d_{gr}) / P$
RMSE	$(\sum d_e - d_{gr} ^2 / P)^{1/2}$
iMAE	$(\sum 1/d_e - 1/d_{gr}) / P$
iRMSE	$(\sum 1/d_e - 1/d_{gr} ^2 / P)^{1/2}$

B. Baselines for Ablation

To perform the ablation study presented in results, we compare our proposed method with the following baselines.

Stereo-based learning (SL): A stereo-based model is introduced into the basic framework, referred to as Baseline, proposed in [21]. The stereo outputs d_s from the stereo-based depth model estimation are used to optimize the distilled depth d_d .

Multi-view Depth Consistency (MC): Based on the basic framework, multi-view adjacent images and their corresponding sparse maps are input into the student model.

The model outputs the corresponding depth outputs $\{d_i\}$, $i \in [t-1, t, t+1]$, which are used to construct the photometric loss.

Multi-scale Minimum Reprojection (MR): Multi-scale reprojection supervision is introduced into the loss function during depth model training with the per-pixel minimum operation.

Our proposed method (Ours): The proposed method combines stereo-based learning (SL), multi-view depth consistency (MC), and multi-scale minimum reprojection (MR) in the basic framework simultaneously.

We perform a comprehensive analysis of each baseline method to determine the contribution of each component to the overall performance of the proposed method.

C. Results

To demonstrate the effectiveness of our proposed method, we perform an ablation study on the KITTI dataset and report the results in Table 2.

Table 2. Evaluation metrics.

Method	MAE	RMSE	iMAE	iRMSE
Baseline	223.021	808.190	0.953	2.300
MR	224.588	816.997	0.943	2.269
MC	222.715	810.013	0.955	2.286
SL	222.177	806.855	0.949	2.280
Ours	221.897	807.063	0.952	2.270

In Table 2, it can be observed that the sub-module methods proposed in this work achieve at least two better metric values than the baseline method, which was trained using the KITTI dataset. Furthermore, the method of incorporating a stereo-based learning model outperforms the baseline method in all four metrics. Figure 4 presents the distribution of the teacher models that are used to construct the distilled depth. The figure shows that the stereo-based learning teacher model contributes to improving the depth accuracy of a significant percentage of pixels, by around 10%. Our proposed method, which incorporates all three sub-module methods, outperforms the baseline method across all metrics and results in significant improvement in the depth maps, as demonstrated in the qualitative comparisons on KITTI.

In Table 3, we present a comparison with several state-of-the-art works, considering both unsupervised learning-based, including AdaFrame, SynthProj, ScaffNet and KNet, and supervised learning-based, such as SS-S2D, DeepLiDAR, ENet, PENet and NLSPN methods. Our proposed method outperforms all unsupervised learning-based methods in all four metrics. Moreover, in Table 4, our method shows great performance among supervised learning-based methods, even outperforming SS-S2D and DeepLiDAR. These results highlight the effectiveness of our proposed method for depth completion and its potential to improve upon existing state-of-the-art methods.

In Fig. 5, we can observe that our proposed method yields depth maps with improved details compared to the baseline method. Specifically, our method effectively improves the

accuracy of depth estimation for various objects such as cars, poles, road lamps, and others. This suggests that our proposed method is capable of capturing more subtle details in the scene and generating more accurate depth maps.

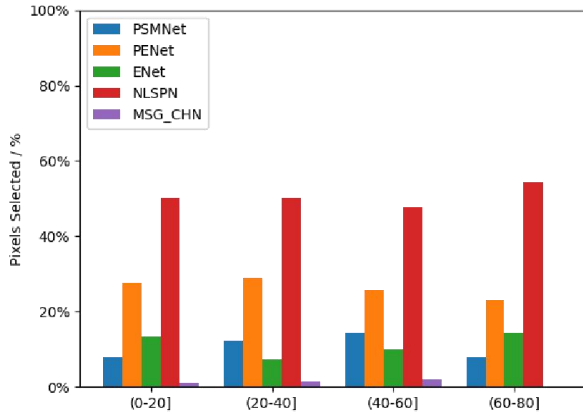


Figure 4. Teacher Model Selection Distribution.

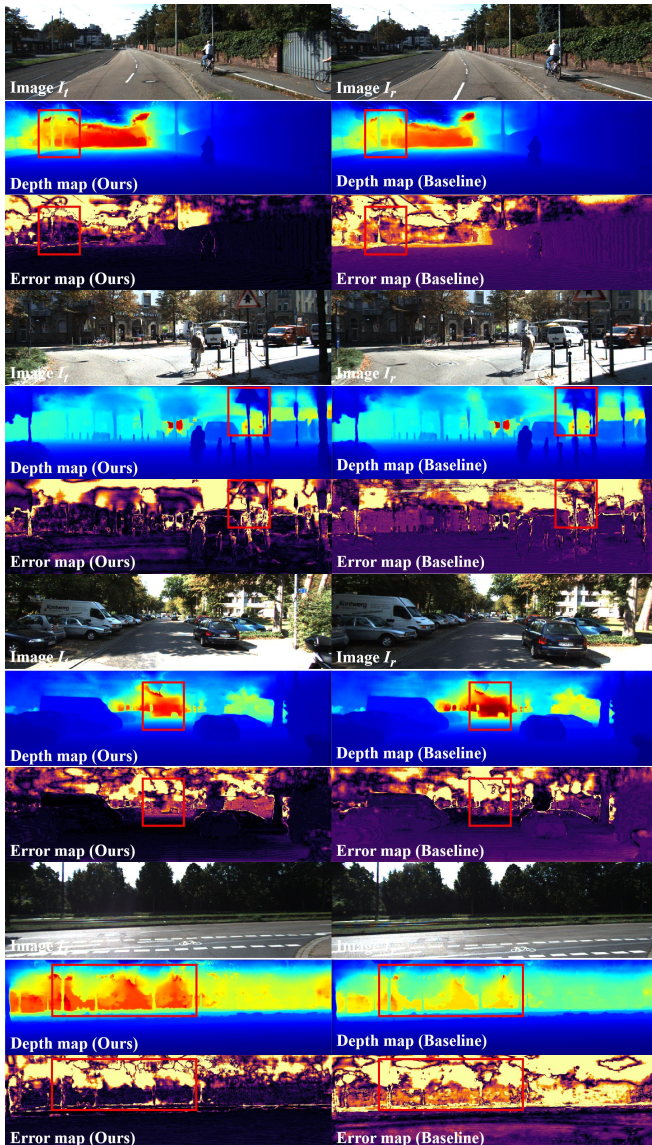


Figure 5. Qualitative comparisons (LHS: the proposed method, RHS: baseline).

Table 3. Unsupervised method comparisons.

Method	MAE	RMSE	iMAE	iRMSE
AdaFrame	291.620	1125.670	1.160	3.320
SynthProj	280.420	1095.260	1.190	3.530
ScaffNet	280.760	1121.930	1.150	3.300
KBNet	256.760	1069.470	1.020	2.950
Ours	221.897	807.063	0.952	2.270

Table 4. Supervised method comparisons.

Method	MAE	RMSE	iMAE	iRMSE
SS-S2D	249.950	814.730	1.210	2.800
DeepLiDAR	226.500	758.380	1.150	2.560
Ours	221.897	807.063	0.952	2.270
ENet	216.260	741.300	0.950	2.140
PENet	210.550	730.080	0.940	2.170
NLSPN	199.590	741.680	0.840	1.990

V. CONCLUSION

The paper proposes a novel depth completion method based on multi-view improved monitored distillation, which generates more accurate depth maps. The method utilizes a publicly available stereo-based model as a teacher model to improve the accuracy of the ensemble distillation. In addition, the proposed method leverages multi-view depth consistency and multi-scale minimum reprojection to provide self-supervised information, which further enhances the accuracy of the depth maps. The advantage of the proposed method is that it takes advantage of existing structure constraints to yield supervised signals for student model training without the need for ground truth information. The experimental results show that the proposed method effectively improves the accuracy of the baseline method of monitored distillation, with a reduction in MAE from 223.021 to 221.897, RMSE from 808.190 to 807.063, iMAE from 0.953 to 0.952, and iRMSE from 2.300 to 2.270. However, the proposed method has limitations in handling some scenes such as high reflectivity, rapidly changing lighting conditions, and transparent objects. These limitations can be addressed in future research.

REFERENCES

- [1] Z. Song, J. Lu, Y. Yao, and J. Zhang, "Self-supervised depth completion from direct visual-LiDAR odometry in autonomous driving," *IEEE Trans. Intelligent Transportation Systems*, vol. 23, no. 8, pp. 11654-11665, 2021.
- [2] F. Ma, L. Carlone, U. Ayaz, and D. Karaman, "Sparse depth sensing for resource-constrained robots," *Int. J. Robotics Research*, vol. 38, no. 8, pp. 935-980, 2019.
- [3] R. Du, E. Turner, M. Dzitsiuk, L. Prasso, I. Duarte, J. Dourgarian, and D. Kim, "DepthLab: Real-time 3D interaction with depth maps for mobile augmented reality," in *Proc. 33rd Annual ACM Symposium on User Interface Software and Technology*, 2020, pp. 829-843.
- [4] H. Laga, L. V. Jospin, F. Boussaid, and M. Bennamoun, "A survey on deep learning techniques for stereo-based depth estimation," *IEEE*

- Trans. Pattern Analysis and Machine Intelligence*, vol. 44, no. 4, pp. 1738-1764, 2020.
- [5] N. Silberman, D. Hoiem, P. Kohli, and R. Fergus, "Indoor segmentation and support inference from rgb-d images," in *Proc. Eur. Conf. Computer Vision (ECCV)*, 2012, pp. 746-760.
 - [6] F. Tian, Y. Gao, Z. Fang, Y. Fang, J. Gu, H. Fujita, and J. N. Hwang, "Depth estimation using a self-supervised network based on cross-layer feature fusion and the quadtree constraint," *IEEE Trans. Circuits and Systems for Video Technology*, vol. 32, no. 4, pp. 1751-1766, 2021.
 - [7] J. Hu, C. Bao, M. Ozay, C. Fan, Q. Gao, H. Liu, and T. L. Lam, "Deep Depth Completion from Extremely Sparse Data: A Survey," *IEEE Trans. Pattern Analysis and Machine Intelligence*, 2022.
 - [8] Z. Huang, J. Fan, S. Cheng, S. Yi, X. Wang, and H. Li, "Hms-net: Hierarchical multi-scale sparsity-invariant network for sparse depth completion," *IEEE Trans. Image Processing*, vol. 29, pp. 3429-3441, 2019.
 - [9] J. Liu, X. Gong, and J. Lin, "Guided inpainting and filtering for kinect depth maps," in *Proc. 21st Int. Conf. Pattern Recognition (ICPR)*, 2012, pp. 2055-2058.
 - [10] J. Uhrig, N. Schneider, L. Schneider, U. Franke, T. Brox, and A. Geiger, "Sparsity invariant cnns," in *Proc. IEEE Int. Conf. 3D Vision (3DV)*, 2017, pp. 11-20.
 - [11] K. Lu, N. Barnes, S. Anwar, and L. Zheng, "Depth completion auto-encoder," in *Proc. IEEE/CVF Winter Conf. Applications of Computer Vision Workshops (WACVW)*, 2022, pp. 63-73.
 - [12] A. Wong, and S. Soatto, "Unsupervised depth completion with calibrated backprojection layers," in *Proc. IEEE/CVF Conf. Computer Vision and Pattern Recognition*, 2021, pp. 12747-12756.
 - [13] S. S. Shivakumar, T. Nguyen, I. D. Miller, S. W. Chen, V. Kumar, and C. J. Taylor, "Dfusenet: Deep fusion of rgb and sparse depth information for image guided dense depth completion," in *Proc. IEEE Intelligent Transportation Systems Conference (ITSC)*, 2019, pp. 13-20.
 - [14] J. Qiu, Z. Cui, Y. Zhang, X. Zhang, S. Liu, B. Zeng, and M. Pollefeys, "Deeplidar: Deep surface normal guided depth prediction for outdoor scene from sparse lidar data and single color image," in *Proc. IEEE/CVF Conf. Computer Vision and Pattern Recognition*, 2019, pp. 3313-3322.
 - [15] X. Cheng, P. Wang, and R. Yang, "Depth estimation via affinity learned with convolutional spatial propagation network," in *Proc. Eur. Conf. Computer Vision (ECCV)*, 2018, pp. 103-119.
 - [16] J. Gu, Z. Xiang, Y. Ye, and L. Wang, "DenseLiDAR: A real-time pseudo dense depth guided depth completion network," *IEEE Robotics and Automation Letters*, vol. 6, no. 2, pp. 1808-1815, 2021.
 - [17] Pilzer, S. Lathuiliere, N. Sebe, and E. Ricci, "Refine and distill: Exploiting cycle-inconsistency and knowledge distillation for unsupervised monocular depth estimation," in *Proc. IEEE/CVF Conf. Computer Vision and Pattern Recognition*, 2019, pp. 9768-9777.
 - [18] C. Godard, O. Mac Aodha, M. Firman, and G. J. Brostow, "Digging into self-supervised monocular depth estimation," in *Proc. IEEE Int. Conf. Computer Vision*, 2019, pp. 3828-3838.
 - [19] C. Godard, O. Mac Aodha, and G. J. Brostow, "Unsupervised monocular depth estimation with left-right consistency," in *Proc. IEEE Conf. Computer Vision and Pattern Recognition (CVPR)*, 2017, pp. 270-279.
 - [20] A. Pilzer, D. Xu, M. Puscas, E. Ricci, and N. Sebe, "Unsupervised adversarial depth estimation using cycled generative networks," in *Proc. IEEE Int. Conf. 3D Vision (3DV)*, 2018, pp. 587-595.
 - [21] T. Y. Liu, P. Agrawal, A. Chen, B. W. Hong, and A. Wong, "Monitored distillation for positive congruent depth completion," in *Proc. Eur. Conf. Computer Vision (ECCV)*, 2022, pp. 35-53.
 - [22] A. Shaked, and L. Wolf, "Improved stereo matching with constant highway networks and reflective confidence learning," in *Proc. IEEE Conf. Computer Vision and Pattern Recognition (CVPR)*, 2017, pp. 4641-4650.
 - [23] A. Kendall, H. Martirosyan, S. Dasgupta, P. Henry, R. Kennedy, A. Bachrach, and A. Bry, "End-to-end learning of geometry and context for deep stereo regression," in *Proc. IEEE Int. Conf. Computer Vision*, 2017, pp. 66-75.
 - [24] C. Won, J. Ryu, and J. Lim, "End-to-end learning for omnidirectional stereo matching with uncertainty prior," *IEEE Trans. Pattern Analysis and Machine Intelligence*, vol. 43, no. 11, pp. 3850-3862, 2020.
 - [25] J. R. Chang, and Y. S. Chen, "Pyramid stereo matching network," in *Proc. IEEE Conf. Computer Vision and Pattern Recognition (CVPR)*, 2018, pp. 5410-5418.
 - [26] A. Wong, X. Fei, S. Tsuei, and S. Soatto, "Unsupervised depth completion from visual inertial odometry," *IEEE Robotics and Automation Letters*, vol. 5, no. 2, pp. 1899-1906, 2020.
 - [27] Y. Yang, A. Wong, and S. Soatto, "Dense depth posterior (ddp) from single image and sparse range," in *Proc. IEEE/CVF Conf. Computer Vision and Pattern Recognition*, 2019, pp. 3353-3362.
 - [28] J. Hu, C. Fan, H. Jiang, X. Guo, Y. Guo, X. Lu, and T. L. Lam, "Boosting light-weight depth estimation via knowledge distillation," *arXiv preprint arXiv:2105.06143*, 2021.
 - [29] Y. Liu, C. Shu, J. Wang, and C. Shen, "Structured knowledge distillation for dense prediction," *IEEE Trans. Pattern Analysis and Machine Intelligence*, 2020.
 - [30] M. Hu, S. Wang, B. Li, S. Ning, L. Fan, and X. Gong, "Penet: Towards precise and efficient image guided depth completion," in *Proc. IEEE Int. Conf. Robot Automation (ICRA)*, 2021, pp. 13656-13662.
 - [31] A. Li, Z. Yuan, Y. Ling, W. Chi, and C. Zhang, "A multi-scale guided cascade hourglass network for depth completion," in *Proc. IEEE/CVF Winter Conf. Applications of Computer Vision Workshops (WACVW)*, 2020, pp. 32-40.
 - [32] J. Park, K. Joo, Z. Hu, C. K. Liu, and I. So Kweon, "Non-local spatial propagation network for depth completion," in *Proc. Eur. Conf. Computer Vision (ECCV)*, 2020, pp. 120-136.